Research Article Vol. 14, No. 10 / 1 Oct 2023 / Biomedical Optics Express 5405
Biomedical Optics EXPRESS

Noninvasive transcutaneous bilirubin measurement in adults using skin diffuse reflectance

CHIA-TE CHEN,[1,2,†] SHENG-HAO TSENG,[3,4,†] BING-HSUAN SUNG,[3] YING-YU CHEN,[3] AND HSIU-CHI CHENG[2,5,6,7,*]

[1]*Department of Nursing, National Cheng Kung University Hospital, College of Medicine, National Cheng Kung University, Tainan, Taiwan*
[2]*Department of Internal Medicine, National Cheng Kung University Hospital, College of Medicine, National Cheng Kung University, Tainan, Taiwan*
[3]*Department of Photonics, National Cheng Kung University, Tainan, Taiwan*
[4]*School of Dentistry, College of Dental Medicine, Kaohsiung Medical University, Kaohsiung, Taiwan*
[5]*Institute of Clinical Medicine, College of Medicine, National Cheng Kung University, Tainan, Taiwan*
[6]*Institute of Molecular Medicine, College of Medicine, National Cheng Kung University, Tainan, Taiwan*
[7]*Department of Internal Medicine, Tainan Hospital, Ministry of Health and Welfare, Tainan, Taiwan*
[†]These authors contributed equally to this work
[*]*teishuki@mail.ncku.edu.tw*

Abstract: Accurate measurement of bilirubin concentration in adults is crucial for the diagnosis and management of liver and biliary tract diseases. Traditional methods relying on central laboratory testing pose challenges such as invasiveness, patient discomfort, and time consumption. Non-invasive alternatives have been explored, but their applicability to adult populations remains uncertain. This study aimed to develop and validate a portable non-invasive optical system based on spatially resolved diffuse reflectance spectroscopy (DRS) specifically tailored for adult transcutaneous bilirubin measurement. Forty-two adult patients with various underlying conditions were included in the study. Comparisons between transcutaneous bilirubin values measured by the DRS system and total serum bilirubin concentrations obtained through blood tests revealed strong correlations, particularly at the neck ($r = 0.872$) and the medial side of the right upper arm ($r = 0.940$). Bland-Altman analyses demonstrated substantial agreement between the transcutaneous bilirubin values and total serum bilirubin concentrations. The results highlight the potential of the non-invasive DRS system as a convenient and reliable tool for monitoring bilirubin values in adults.

1. Introduction

Jaundice, or hyperbilirubinemia, is a quite common clinical condition, and can be classified as unconjugated or conjugated. In adults, the major pathophysiologic conditions leading to conjugated hyperbilirubinemia include hepatocellular injury, intrahepatic cholestasis, and extrahepatic biliary duct obstruction. Liver cirrhosis and acute hepatitis, commonly caused by viral hepatitis B or C infection, alcohol consumption, or non-alcoholic fatty liver disease, are prevalent global conditions resulting in hepatocellular injury [1]. Mortality rates associated with liver cirrhosis have been high, with cirrhosis-related deaths in the global total death increasing from 1.9% (1.8%–2.0%) in 1990 to 2.4% (2.3%–2.6%) in 2017 [2]. Biliary duct obstruction, due to biliary stones or cancers, remains a significant burden, with prevalence rates of cholelithiasis and choledocholithiasis estimated to be around 10% to 20% worldwide [3]. Although mortality rates related to gallstone-related diseases have shown a gradual decline due to advances in diagnosis and care, incidence and mortality rates of gallbladder and biliary tract cancer have increased [4]. Consequently, the diagnosis of jaundice remains important in clinical practice.

#500833 https://doi.org/10.1364/BOE.500833
Journal © 2023 Received 18 Jul 2023; revised 17 Sep 2023; accepted 18 Sep 2023; published 25 Sep 2023

Biomedical Optics EXPRESS

Jaundice is characterized by tea-colored urine and the presence of icteric skin and sclera. Traditionally, the assessment of jaundice relies on measuring total serum bilirubin through central laboratory testing, which involves phlebotomy and poses challenges such as time consumption, patient anxiety, pain, and an increased risk of infection. Consequently, the development of non-invasive methods to measure bilirubin concentration has emerged as an alternative approach.

Transcutaneous bilirubin can be determined by analyzing the light reflected by skin and subcutaneous tissues. Previous studies by Yamanouchi et al. and Bosschaart et al. have demonstrated the use of non-invasive devices for assessing transcutaneous bilirubin, showing a strong correlation with total serum bilirubin concentration in neonatal jaundice [5–7]. However, these devices were primarily validated in neonates with total serum bilirubin concentration ranging from 5.85–11.7 mg/dL [7]. Since healthy adults typically have serum bilirubin concentration below 1.2 mg/dL, it remains uncertain whether these devices are applicable for adults. Point-of-care testing (POCT) has emerged as a convenient monitoring tool that provides rapid laboratory results in clinical practice [8,9]. Commercial transcutaneous bilirubinometers, such as the Dräger Jaundice Meter JM-105 (Drägerwerk AG & Co. KGaA, Lübeck, Germany) and BiliChek (Philips, Amsterdam, Netherlands) noninvasive bilirubin assessment tool, are exclusively approved for use in newborns [10,11]. Therefore, the correlation between transcutaneous bilirubin values measured by such devices and total serum bilirubin concentrations in adults remains uncertain.

Diffuse reflectance spectroscopy (DRS) is a well-established non-invasive method widely used in biomedical optics. It encompasses three variants: spatially resolved diffuse reflectance spectroscopy, frequency domain diffuse reflectance spectroscopy, and time-resolved diffuse reflectance spectroscopy [12–14]. Among these variants, spatially resolved diffuse reflectance spectroscopy is relatively easy to implement. It involves delivering steady-state light into the target tissue at various source-to-detector separations to collect diffuse reflectance spectra. From these spectra, the absorption coefficient and reduced scattering coefficient of the target tissue can be calculated using a proper photon transport model [6,12]. The tissue composition can then be derived based on the assumption that tissues consist of specific chromophores, and their light absorption follows the Beer-Lambert's law in a superposition manner [13,15,16]. Spatially resolved diffuse reflectance spectroscopy is particularly suitable for measuring skin tissues due to its simple structure, low cost, portability, and suitability for superficial tissue measurement with source-to-detector separations of less than 5 mm. Our group has successfully utilized spatially resolved diffuse reflectance spectroscopy in various applications, including non-contact measurement for skin collagen [17] and evaluation of treatment response in keloids [18].

In a previous study, we demonstrated a custom spatially resolved diffuse reflectance spectroscopy (DRS) system capable of measuring transcutaneous bilirubin in newborns. The system accurately recovers transcutaneous bilirubin values highly correlated with total serum bilirubin concentrations [19]. This spatially resolved diffuse reflectance spectroscopy system determines the absorption and scattering properties of the skin, utilizing the recovered skin absorption spectrum to extract the bilirubin value. This method minimizes interference from different skin scattering properties and chromophore compositions among subjects. However, adults generally have darker skin and different skin compositions, potentially complicating the contribution of bilirubin pigment in the detected light reflectance. Thus, this study aimed to verify the capability of the spatially resolved diffuse reflectance spectroscopy system in measuring transcutaneous bilirubin in adults and validate the correlation between the transcutaneous bilirubin values and total serum bilirubin concentrations determined through blood tests.

Biomedical Optics EXPRESS

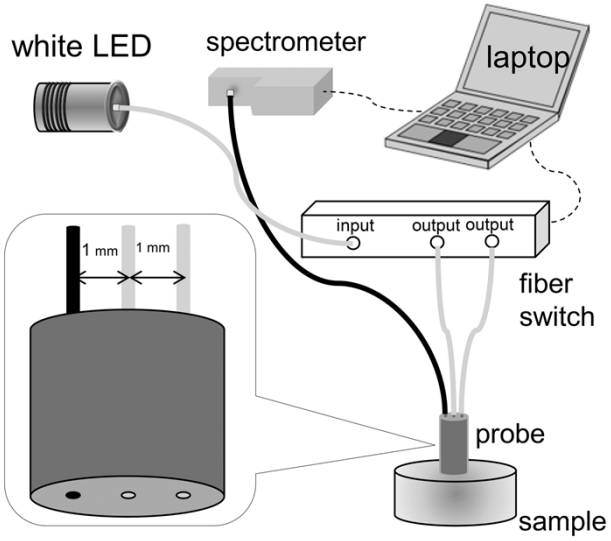

Fig. 1. Schematic setup of the spatially resolved diffuse reflectance spectroscopy system employed in this study. The system consisted of a white LED, a spectrometer, a fiber switch, a fiber probe, and a laptop computer. Lower left shows the detail configuration of the fiber probe.

2. Methods

2.1. Configuration of the portable diffuse reflectance measurement system

In the spatially resolved DRS system, we employed a custom-designed optical fiber probe to collect spatially resolved reflectance from the skin of subjects (Fig. 1). The probe consisted of optical fibers with a core diameter of 440 µm and a numerical aperture of 0.22. Of the fibers in the probe, two were connected to the light source through an optical switch (Piezosystem Jena, Germany), whereas the remaining fiber served as the detector fiber. The detector fiber was connected to a spectrometer (QE65000, Ocean Optics, FL, USA) for detecting the optical reflectance signal. For illumination, a white-light light-emitting diode (LED, MCWHL5-6500 K, Thorlabs, USA) emitting a broad spectrum ranging from 400 to 600 nm was employed. The spectrometer and optical switch were linked to a laptop computer and controlled using a custom MATLAB program (MathWorks, Natick, MA, USA). Spatially resolved DRS leverages mathematical models, such as diffusion theory or Monte Carlo simulations, to interpret how light interacts within tissue. To effectively constrain the parameters of these models and achieve an optimal fit with the observed data, measurements from multiple source-detector pairs are essential. While traditional spatially resolved DRS setups often require data from more than two such pairs, our tailored model has been optimized to extract accurate tissue optical properties using just two source-to-detector separations: 1 mm and 2 mm. The dual-detector configuration not only streamlines the data collection process but also allows for a more compact optical fiber probe design. This compactness is particularly advantageous in clinical settings, facilitating easy operation and minimizing patient discomfort. In addition, we employed a calibration procedure akin to the one used in our prior study [18]. Each set of skin reflectance spectra, along with the system's dark noise, was calibrated using reflectance spectra obtained from a siloxane phantom with known optical properties ($\mu_a = 0.07\ mm^{-1}$ and $\mu_s' = 1.91\ mm^{-1}$ at 780 nm). This process effectively removed the instrument's response. By utilizing this specially designed optical fiber probe and a combination of the light source, spectrometer, and optical switch, our system enabled

Biomedical Optics EXPRESS

the acquisition of spatially resolved reflectance measurements from the skin. The measurement results were subsequently utilized in calculations of skin absorption spectra, which were vital for accurate bilirubin assessment.

2.2. Theoretical models

While spatially resolved DRS is inherently model-based, the transformation of measured diffuse reflectance into tissue optical properties isn't a straightforward fitting operation. Spatially resolved DRS necessitates a robust nonlinear mathematical model to accurately map measured diffuse reflectance to tissue optical properties. The diffusion theory, a common approach for deducing optical properties in tissues, does indeed have constraints. Specifically, it may not be as reliable for measurements with source-to-detector separations under 5 mm. This is because the diffusion approximation presumes the tissue to be both semi-infinite and uniform. It is most precise when the photon transport is dominated by multiple scattering events. At shorter source-to-detector separations, there might not be sufficient scattering events for the diffusion theory to be applicable. In our prior research, we pioneered an artificial neural network (ANN) model specifically designed to deduce skin absorption and reduced scattering spectra from diffuse reflectance, gathered at source-to-detector separations of 1 and 2 mm. The construction and validation of this model were described in the previous studies in detail [20]. Briefly, we designed an artificial neural network architecture consisting of an input layer, two hidden layers, and an output layer to model the relationship between diffuse reflectance and skin optical properties. The size of the neurons in the two hidden layers was set to 10. The artificial neural network model was trained using the MATLAB (MathWorks, USA) function "trainNetwork" to relate 3600 combinations of absorption and reduced scattering coefficients to the corresponding Monte Carlo simulated diffuse reflectance at 1 and 2 mm. In the Monte Carlo simulations, we modeled the turbid medium with a semi-infinite geometry. The simulations encompassed a broad spectrum of optical properties pertinent to human skin at wavelengths between 450 and 550 nm. Specifically, absorption coefficients (μ_a) ranged from 0.01 to 2 mm^{-1}, and scattering coefficients (μ_s') spanned from 0.1 to 5 mm^{-1}. The *in-vivo* skin absorption spectrum was derived using the artificial neural network model, which was then utilized to quantify the skin bilirubin value by applying the Beer-Lambert law as follows [21]:

$$\begin{aligned}\mu_{a(skin)}(\lambda) = 2.303\times[&C_{HbO_2}\times\varepsilon_{HbO_2}(\lambda) + C_{Hb}\times\varepsilon_{Hb}(\lambda)\\ &+ C_{melanin}\times\varepsilon_{melanin}(\lambda)\\ &+ C_{bilirubin}\times\varepsilon_{bilirubin}(\lambda)]\end{aligned} \quad (1)$$

where C and ε represent the concentration and the extinction coefficient of a certain substance, respectively. For the chromophore extinction coefficients, we relied on online data from the Oregon Medical Laser Center [22]. Equation (1) establishes a relationship between the skin absorption spectrum and the concentrations of skin chromophores, namely hemoglobin, melanin, and bilirubin. Given that the exact concentrations of these chromophores remain undetermined, the problem becomes one of optimization. To address this, we employed the MATLAB function "lsqcurvefit" to deduce the concentrations of hemoglobin, melanin, and bilirubin.

The raw bilirubin values obtained through our diffuse reflectance spectroscopy technique represent the bilirubin present in the extravascular space and are not directly equivalent to the total serum bilirubin concentrations. Besides, it is noteworthy that Eq. (1) inherently presents a linear relationship, implying that the raw skin bilirubin value has a direct linear dependence on the skin absorption spectrum. Moreover, under the assumption that the serum bilirubin concentration linearly influences the magnitude of skin absorption, there exists a linear relationship between the raw skin bilirubin value and the serum bilirubin concentration. Therefore, a conversion process was necessary to establish a relationship between the raw bilirubin values and the total serum bilirubin concentrations. To achieve this, a linear regression analysis was performed between

Biomedical Optics EXPRESS

the raw bilirubin values and the total serum bilirubin concentrations at each measurement site. This enabled the mapping of the raw bilirubin values (μM) to the corresponding transcutaneous bilirubin concentrations (mg/dL) using the linear regression formula specific to each site.

2.3. Study design and patient enrollment for measurement of transcutaneous bilirubin

The measurement of transcutaneous bilirubin was conducted at the inpatient ward of the National Cheng Kung University Hospital in Tainan, Taiwan. Prospective enrollment was carried out for patients aged 20 years and above, admitted to the Division of General Internal Medicine, Department of Internal Medicine, from January 2021 to July 2022. Ethical approval for this study was obtained from the National Cheng Kung University Hospital Institutional Review Board (approval Number: B-ER-109-354). The date of approval was Dec. 28, 2020. Written informed consents were obtained from all enrolled patients.

Patient characteristics and clinical data were carefully recorded. Serum bilirubin concentrations were determined through phlebotomy using the Cobas 8000 Modular Analyzer Series c502 (Roche Diagnostics, Switzerland). The clinical laboratory technologists involved in the central laboratory analysis were blinded to the patients' data and the results of transcutaneous bilirubin measurement. Within 3 hours after phlebotomy, two investigators, who were also blinded to the data, performed transcutaneous bilirubin measurement at five specified sites: the forehead, cheek, neck, and medial side of the left and right upper arm, using our portable DRS system. The measurement site on the forehead lies at the midpoint between the hairline and the middle eyebrows. The site on the cheek lies at the midpoint between the nostril and the ipsilateral earlobe. The site on the neck lies at the point between the sternocleidomastoid muscle and the trapezius muscle at the horizontal level of the cricoid cartilage. The site on the upper arm is at the midpoint of the medial side between the shoulder and the elbow. Three measurements were obtained at each site to assess the percent difference between measurements. If the percentage difference between measurements at a particular site exceeded 5%, the measurement at that site was repeated. Areas with intravenous sets, scars, nevi, melasma, seborrheic keratosis, and/or other skin pigmentation were excluded from measurement. The derived bilirubin values obtained from the portable DRS system were compared with the total serum bilirubin concentrations obtained through phlebotomy.

3. Statistical analysis

The correlation between transcutaneous bilirubin values and total serum bilirubin concentrations was analyzed using linear regression analyses. Furthermore, Bland-Altman plots were employed to assess the bias and 95% limits of agreement (LOA) between the transcutaneous bilirubin values and total serum bilirubin concentrations.

4. Results

4.1. Demographic features of the patients

A total of 42 patients were included in the study, of which 24 (57.1%) were female. The demographic characteristics of the patients were as follows: the median age was 70.5 years (25th–75th interquartile range: 63.0–82.25 years), ranging from 30 to 92 years. The median body height was 157.5 cm (25th–75th interquartile range: 151.8–165 cm), ranging from 135 to 180 cm. The median body weight was 59 kg (25th–75th interquartile range: 48–70.3 kg), ranging from 35 to 93 kg. The median total serum bilirubin concentration was 0.55 mg/dL (25th–75th interquartile range: 0.3–1.1 mg/dL), ranging from 0.1 to 3.9 mg/dL. The enrolled patients had various underlying conditions, including urinary tract infection/acute pyelonephritis in 11 (26.2%) patients, common bile duct stone/acute cholangitis in 7 (16.7%) patients, acute cholecystitis in 5 (11.9%) patients, acute hepatitis in 3 (7.1%) patients, pneumonia in 3 (7.1%)

Biomedical Optics EXPRESS

patients, cellulitis in 3 (7.1%) patients, sepsis in 2 (4.8%) patients, colitis in 2 (4.8%) patients, cirrhosis in 2 (4.8%) patients, liver abscess in 2 (4.8%) patients, uremia in 1 (2.4%) patient, and duodenal ulcer in 1 (2.4%) patient. It is important to note that none of the patients experienced any adverse events following phlebotomy or during the transcutaneous bilirubin measurement process. Additionally, in this study, the mean melanin concentration determined using our DRS system for the left upper arm was 0.76%, with a standard deviation of 0.46%. For context, in a previous study we conducted [16], the upper arm's average melanin concentration for the skin type III-IV group was 1.66%.

4.2. Comparisons between transcutaneous bilirubin values and total serum bilirubin concentrations

The transcutaneous bilirubin values converted from the raw bilirubin values were compared with the corresponding total serum bilirubin concentrations obtained from the central laboratory using linear regression analyses. Here we detailed the linear regression parameters for the raw bilirubin values in relation to the total serum bilirubin concentrations across the five measurement sites. For the forehead, the slope was 3.63 and the intercept was −2.56. For the cheek, the slope was 2.88 and the intercept was −1.35. In the case of the neck, the slope was 2.06 with an intercept of −1.24. For the left upper arm, the slope was 4.54 and the intercept was −1.56. Lastly, for the right upper arm, the slope was 2.65 and the intercept was −0.80. Patients with intravenous sets or skin pigmentation at certain measurement sites were excluded from the transcutaneous bilirubin measurement. The correlation coefficients (r) between transcutaneous bilirubin values and total serum bilirubin concentrations were 0.609 at the site on the forehead, 0.800 at the cheek, 0.872 at the neck, 0.538 at the medial side of the left upper arm, and 0.940 at the medial side of the right upper arm (Fig. 2(a)–(e)). These findings indicate a significant association between the transcutaneous bilirubin values and total serum bilirubin concentrations, supporting the validity of the non-invasive DRS measurement method.

To further assess the agreement between transcutaneous bilirubin values and total serum bilirubin concentrations, Bland-Altman analyses were performed. The bias (95% LOA) values were determined as follows: -1.884×10^{-4} (−2.534–2.533) mg/dL at the site on the forehead, -1.200×10^{-4} (−1.440–1.440) mg/dL at the cheek, -9.528×10^{-5} (−0.997–0.996) mg/dL at the neck, -3.018×10^{-5} (−3.194–3.194) mg/dL at the medial side of the left upper arm, and 1.583×10^{-5} (−0.729–0.729) mg/dL at the medial side of the right upper arm (Fig. 3(a)–(e)). These results indicate a substantial level of agreement between transcutaneous bilirubin values and total serum bilirubin concentrations, supporting the potential utility and accuracy of the transcutaneous bilirubin measurement method.

4.3. Site dependent transcutaneous bilirubin and total serum bilirubin correlation coefficients

The correlation coefficients between transcutaneous bilirubin values and total serum bilirubin concentrations varied across different measurement sites. As depicted in Fig. 2, the correlations were relatively high at the site on the neck, but low at the forehead. Similarly, the correlations were high at the right upper arm but low at the left upper arm. Notably, we observed a subject (No. 029) whose transcutaneous bilirubin value aligned closely with the linear regression line at the neck but deviated from the line at the forehead (the dot in the red square on Fig. 2(c) and 2(a), respectively).

To investigate this discrepancy, we analyzed the difference between the recovered skin absorption spectrum and the best chromophore fitting spectrum for subject No. 029, based on Eq. (1). At the site on the neck, the best chromophore fitting spectrum (red dotted line) exhibited good agreement with the skin absorption spectrum (black line) at the wavelength range between 500 to 540 nm (the red circle in Fig. 4(a)). However, at the site on the forehead, the agreement

Biomedical Optics EXPRESS

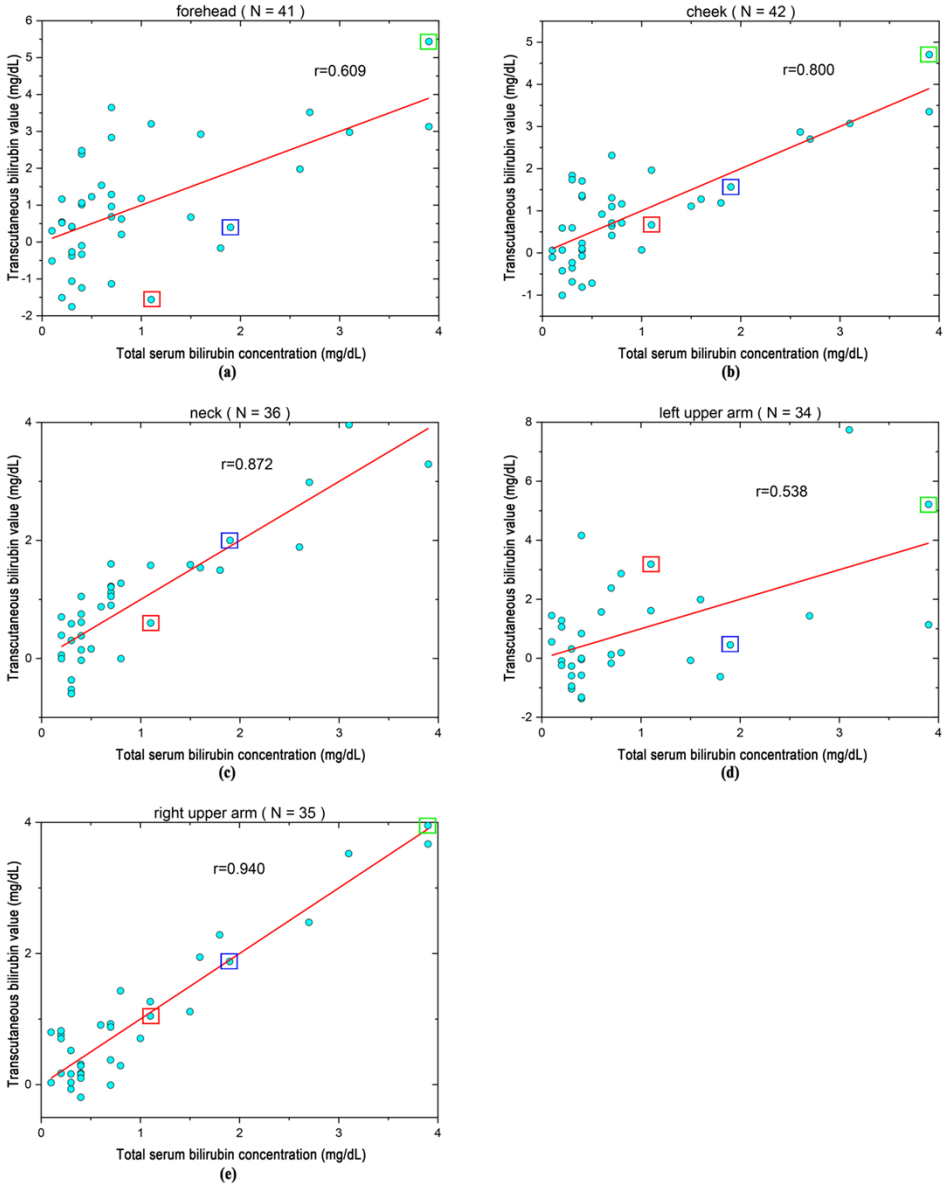

Fig. 2. Correlation plots comparing transcutaneous bilirubin values (measured using DRS) with total serum bilirubin concentrations (obtained from blood tests) at five measurement sites: (a) forehead, (b) cheek, (c) neck, (d) medial side of the left upper arm, and (e) medial side of the right upper arm.

Biomedical Optics EXPRESS

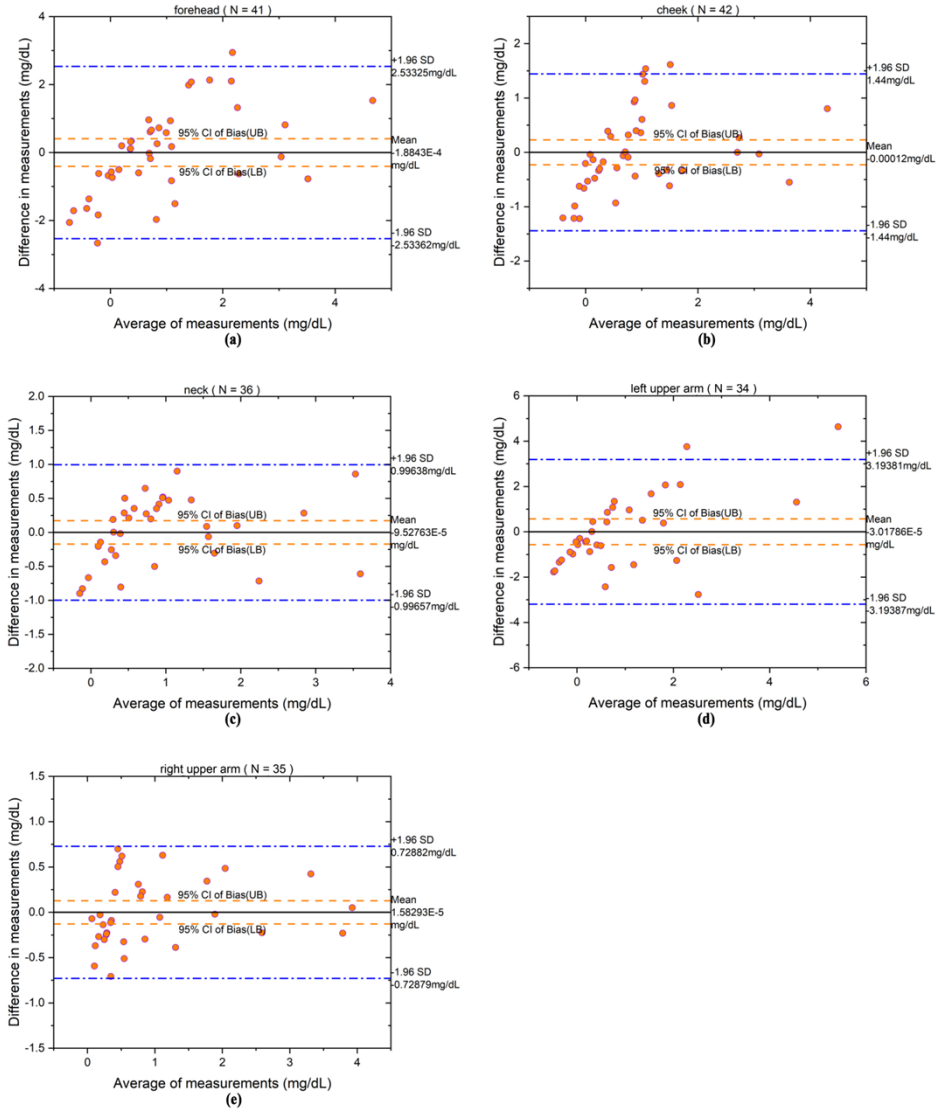

Fig. 3. Bland-Altman plots showing the bias and 95% limits of agreement between transcutaneous bilirubin values and total serum bilirubin concentrations at the five measurement sites: (a) forehead, (b) cheek, (c) neck, (d) medial side of the left upper arm, and (e) medial side of right upper arm.

Biomedical Optics EXPRESS

between the best chromophore fitting spectrum and the skin absorption spectrum was only fair (the red circle in Fig. 4(b)). The percentage deviation of the best chromophore fitting spectrum from the skin absorption spectrum was calculated, revealing a deviation of approximately ±1% at the neck, whereas it was approximately ±3% at the forehead.

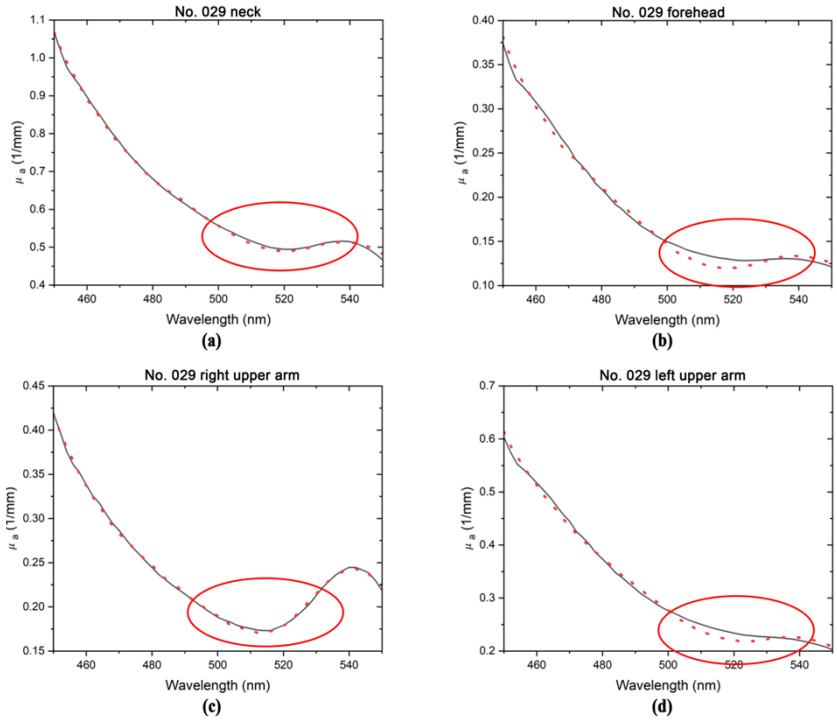

Fig. 4. The analysis of fitting quality for subject No. 029, depicting the recovered skin absorption spectrum (black line) and the best chromophore fitting spectrum (red dotted line) at various measurement sites: neck (a), forehead (b), right upper arm (c), and left upper arm (d).

Additionally, subjects No. 027, 029, and 039 consistently exhibited the transcutaneous bilirubin values that closely followed the linear regression line at the site on the right upper arm but deviated from the line at the left upper arm (the dots in the blue [No. 027], red [No. 029], and green [No. 039] squares on Fig. 2(e) and 2(d), respectively). The chromophore fitting quality of subject No. 029 was analyzed and demonstrated good agreement between the best chromophore fitting spectrum (red dotted line) and the skin absorption spectrum (black line) at the right upper arm (the red circle in Fig. 4(c)), whereas the agreement was only fair at the left upper arm (the red circle in Fig. 4(d)). The percentage deviation of the best chromophore fitting spectrum from the skin absorption spectrum revealed a deviation of approximately ±1% at the right upper arm, whereas it was approximately ±2% at the left upper arm. The chromophore fitting quality of No. 027 and 039 was also analyzed and demonstrated similar results (figures not shown).

These findings indicated that the correlations between transcutaneous bilirubin values and total serum bilirubin concentrations were influenced by the quality of chromophore fitting to the skin absorption spectra at different measurement sites. The results emphasized the site-dependent nature of transcutaneous bilirubin measurement and highlighted the importance of considering individual variations when interpreting the data.

Biomedical Optics EXPRESS

5. Discussion

While commercial non-invasive transcutaneous bilirubinometers are available, they are approved only for checking neonatal jaundice. Characteristics of jaundice differ between newborns and adults. Neonatal jaundice primarily involves unconjugated hyperbilirubinemia, whereas adult jaundice predominantly stems from conjugated hyperbilirubinemia due to hepatocellular injury or extrahepatic biliary duct obstruction. Furthermore, unique features of the newborn skin, such as its smoothness, lack of pigmentation, and absence of wrinkles, differ from those of the adult skin, which are rough, freckled, cracked, and wrinkled. To the best of our knowledge, we have not found any relevant reports on non-invasive transcutaneous bilirubinometers for adults.

This study demonstrated the effectiveness of a portable DRS system in combination with an advanced spectral analysis algorithm for accurately assessing adult transcutaneous bilirubin values. The findings revealed a substantial correlation between transcutaneous bilirubin measurements and total serum bilirubin concentrations, particularly when evaluating the skin on the neck or medial side of the right upper arm in adults.

The correlation coefficient r and the mean bias (95% LOA) were 0.940 and 1.583×10^{-5} (−0.729–0.729) mg/dL, respectively, at the medial side of the right upper arm (Fig. 2(e) and 3(e)) and 0.872 and -9.528×10^{-5} (−0.997–0.996) mg/dL, respectively, at the neck (Fig. 2(c) and 3(c)). In comparison, Radfar et al. used BiliChek to measure neonatal jaundice and reported a correlation coefficient of 0.929 and a mean bias (95% LOA) of 0.65 (−1.8–3.1) mg/dL between transcutaneous bilirubin values and total serum bilirubin concentrations [23]. Kuang et al. used the Werfen GEM 4000 blood gas analyzer to measure neonatal bilirubin and found a mean bias (95% LOA) of 0.77 (−0.26–1.79) mg/dL compared to the automatic biochemical analyzer [24]. Our DRS system exhibited low mean bias and 95% LOA. The performance was attributed to the use of an artificial neural network that effectively separated the absorption and scattering properties of the skin and combined it with the Beer-Lambert's law-based chromophore fitting to differentiate between hemoglobin, melanin, and bilirubin, resulting in reliable bilirubin measurement. On the other hand, Polley et al. developed an optical device for bilirubin monitoring, employing a non-contact probe that collected reflectance light through the human conjunctiva [25]. Their results revealed a high correlation coefficient of 0.96 between the bilirubin values derived from the optical system and those from blood tests, with a mean bias (95% LOA) of −0.06 (−0.42–0.30) mg/dL. However, it is crucial to acknowledge that this method carries potential risks of eye injury since it involves exposing the eyeball to direct light. Additionally, the collected diffused light from the "non-contact" probe could be susceptible to interference from ambient light sources, which may affect the accuracy and reliability of the measurement.

The forehead and sternum are the two standard measurement sites for neonatal transcutaneous bilirubinometry; however, which measurement site had higher predictive bilirubin concentrations in adults was uncertain. Therefore, we selected the forehead, cheek, neck, and medial sites of bilateral upper arms but not the sternum for transcutaneous bilirubin measurement in adults. These sites are different from those in neonatal measurement except the forehead because of concerns about privacy, pigmented skin after sun exposure or stasis dermatitis, and body hair in adults. This study revealed variations in the correlation between transcutaneous bilirubin values and total serum bilirubin concentrations across different measurement sites. We observed higher correlations at the right upper arm and neck, while there were lower correlations at the forehead and left upper arm. Inherent biological variability may play a role in the observed differences. We propose that these differences may be attributed to variations in skin conditions at each site, although the unique nature of this occurrence remains uncertain. To validate and replicate our findings, further studies involving a larger population are warranted.

This study has some limitations. First, the theoretical model used in this study assumed that the target tissue was homogeneous, whereas human tissue is not. Therefore, the measurement results

Biomedical Optics EXPRESS

of our system may be influenced by the diffusion of serum bilirubin to the extravascular space and may not reflect instantaneous variations in serum bilirubin. Second, the subjects recruited in this study had serum bilirubin concentrations ranging from 0.1–3.9 mg/dL. Further studies are required to validate the performance of the non-invasive transcutaneous bilirubinometer for subjects with bilirubin concentrations exceeding 5 mg/dL. Third, we did neither compare the measurements under different exerted probe pressure on the skin nor compare the data with commercial transcutaneous bilirubinometers.

The modified Child-Pugh classification is a scoring system used to evaluate the severity of liver disease [26]. The classification has five parameters, including ascites, bilirubin, albumin, prothrombin time, and encephalopathy. Among these parameters, bilirubin stands out as a reliable biomarker unaffected by medication or supplemental interventions like albumin or plasma. Consequently, bilirubin serves as a valuable indicator of disease progression or regression in liver decompensation, whether in acute exacerbation or chronic cirrhosis. When total serum bilirubin concentrations ranged from 1 mg/dL to 3.9 mg/dL, our system could predict bilirubin concentrations well; thus, clinicians got a score of 2 or 3 to calculate the total Child-Pugh score. When total serum bilirubin concentrations were less than 1 mg/dL, the prediction was not so well; nevertheless, the predictive concentrations were all < 1 mg/dL. It provided adequate information for clinicians to know a patient having a score of 1 for the modified Child-Pugh classification (Fig. 2(c) and 2(e)).

Telemedicine has made significant strides in recent years, expanding access to healthcare services worldwide [27]. We anticipate that tele-monitoring, alongside virtual visits, will become a routine practice post-COVID-19 pandemic [28]. In this study, we successfully developed an optical system for measuring bilirubin concentrations in adults. It is a non-invasive device that could minimize emotional stress, physical pain, and needle-stick injuries [29]. Moreover, this system could be further developed into a point-of-care testing (POCT) device, providing timely and remote data when combined with communication technologies and requiring minimal staff training [30]. Given the global prevalence of liver and biliary tract diseases, our portable non-invasive transcutaneous bilirubinometer holds potential for widespread application.

6. Conclusion

In conclusion, our study demonstrated a strong correlation between transcutaneous bilirubin measurements and total serum bilirubin concentrations in adults when assessing the skin at the neck ($r = 0.872$) or medial side of the right upper arm ($r = 0.940$). Notably, our system exhibited low mean bias and narrower 95% limits of agreement. This can be attributed to the integration of an artificial neural network and the Beer-Lambert's law-based chromophore fitting, enabling accurate differentiation of hemoglobin, melanin, and bilirubin in the skin. The development of this non-invasive optical system holds great potential in clinical practice, offering a convenient and reliable tool for monitoring bilirubin values in adults. Future studies should aim to validate its performance with a larger and more diverse population to establish its generalizability and expand its clinical utility in liver and biliary tract diseases.

Funding. National Science and Technology Council (NSTC 112-2327-B-006-008); National Cheng Kung University Hospital (NCKUH-11008016, NCKUH-11108003).

Acknowledgments. The authors thank the nurses at the Division of General Internal Medicine, Department of Internal Medicine, National Cheng Kung University Hospital for help conducting this work.

Disclosures. The authors declare no conflicts of interest related to this article.

Data availability. Data underlying the results presented in this paper are not publicly available at this time but may be obtained from the authors upon reasonable request.

Biomedical Optics EXPRESS

References

1. P. Ginès, A. Krag, J. G. Abraldes, E. Solà, N. Fabrellas, and P. S. Kamath, "Liver cirrhosis," Lancet **398**(10308), 1359–1376 (2021).
2. GBD 2017 Cirrhosis Collaborators, "The global, regional, and national burden of cirrhosis by cause in 195 countries and territories, 1990-2017: a systematic analysis for the Global Burden of Disease Study 2017," Lancet Gastroenterol. Hepatol. **5**(3), 245–266 (2020).
3. T. Wilkins, E. Agabin, J. Varghese, and A. Talukder, "Gallbladder dysfunction: cholecystitis, choledocholithiasis, cholangitis, and biliary dyskinesia," Prim. Care **44**(4), 575–597 (2017).
4. G. Ouyang, Q. Liu, Y. Wu, Z. Liu, W. Lu, S. Li, G. Pan, and X. Chen, "The global, regional, and national burden of gallbladder and biliary tract cancer and its attributable risk factors in 195 countries and territories, 1990 to 2017: a systematic analysis for the Global Burden of Disease Study 2017," Cancer **127**(13), 2238–2250 (2021).
5. I. Yamanouchi, Y. Yamauchi, and I. Igarashi, "Transcutaneous bilirubinometry: preliminary studies of noninvasive transcutaneous bilirubin meter in the Okayama National Hospital," Pediatrics **65**(2), 195–202 (1980).
6. N. Bosschaart, R. Mentink, J. H. Kok, T. G. van Leeuwen, and M. C. Aalders, "Optical properties of neonatal skin measured in vivo as a function of age and skin pigmentation," J. Biomed. Opt. **16**(9), 097003 (2011).
7. N. Bosschaart, J. H. Kok, A. M. Newsum, D. M. Ouweneel, R. Mentink, T. G. van Leeuwen, and M. C. G. Aalders, "Limitations and opportunities of transcutaneous bilirubin measurements," Pediatrics **129**(4), 689–694 (2012).
8. J. A. Goble and P. T. Rocafort, "Point-of-Care Testing," J. Pharm. Pract. **30**(2), 229–237 (2017).
9. J. Dalton, "Communications with lab and POCT users," Pract. Lab. Med. **25**, e00223 (2021).
10. U. Costa-Posada, A. Concheiro-Guisán, M. F. Táboas-Ledo, E. González-Colmenero, M. L. González-Durán, M. Suarez-Albo, C. D. Fernández-Feijoo, M. Pumarada-Prieto, C. Martínez-Reglero, and J. R. Fernández-Lorenzo, "Accuracy of transcutaneous bilirubin on covered skin in preterm and term newborns receiving phototherapy using a JM-105 bilirubinometer," J. Perinatol. **40**(2), 226–231 (2020).
11. S. N. el-Beshbishi, K. E. Shattuck, A. A. Mohammad, and J. R. Petersen, "Hyperbilirubinemia and transcutaneous bilirubinometry," Clin. Chem. **55**(7), 1280–1287 (2009).
12. R. M. Doornbos, R. Lang, M. C. Aalders, F. W. Cross, and H. J. Sterenborg, "The determination of in vivo human tissue optical properties and absolute chromophore concentrations using spatially resolved steady-state diffuse reflectance spectroscopy," Phys. Med. Biol. **44**(4), 967–981 (1999).
13. T. H. Pham, O. Coquoz, J. B. Fishkin, E. Anderson, and B. J. Tromberg, "Broad bandwidth frequency domain instrument for quantitative tissue optical spectroscopy," Rev. Sci. Instrum. **71**(6), 2500–2513 (2000).
14. A. Pifferi, J. Swartling, E. Chikoidze, A. Torricelli, P. Taroni, A. Bassi, S. Andersson-Engels, and R. Cubeddu, "Spectroscopic time-resolved diffuse reflectance and transmittance measurements of the female breast at different interfiber distances," J. Biomed. Opt. **9**(6), 1143–1151 (2004).
15. S. H. Tseng, C. K. Hsu, J. Y. Lee, S. Y. Tzeng, W. R. Chen, and Y. K. Liaw, "Noninvasive evaluation of collagen and hemoglobin contents and scattering property of in vivo keloid scars and normal skin using diffuse reflectance spectroscopy: pilot study," J. Biomed. Opt. **17**(7), 077005 (2012).
16. S. H. Tseng, P. Bargo, A. Durkin, and N. Kollias, "Chromophore concentrations, absorption and scattering properties of human skin in-vivo," Opt. Express **17**(17), 14599–14617 (2009).
17. S. Y. Tzeng, T. Y. Kuo, S. B. Hu, Y. W. Chen, Y. L. Lin, K. Y. Chu, and S. T. Tseng, "Skin collagen can be accurately quantified through noninvasive optical method: Validation on a swine study," Skin Res. Technol. **24**(1), 59–64 (2018).
18. C. K. Hsu, S. Y. Tzeng, C. C. Yang, J. Y. Y. Lee, L. L. H. Huang, W. R. Chen, M. Hughes, Y. W. Chen, Y. K. Liao, and S. H. Tseng, "Non-invasive evaluation of therapeutic response in keloid scar using diffuse reflectance spectroscopy," Biomed. Opt. Express **6**(2), 390–404 (2015).
19. N. Y. Cheng, Y. L. Lin, M. C. Fang, W. H. Lu, C. C. Yang, and S. H. Tseng, "Noninvasive transcutaneous bilirubin assessment of neonates with hyperbilirubinemia using a photon diffusion theory-based method," Biomed. Opt. Express **10**(6), 2969–2984 (2019).
20. Y. W. Chen and S. H. Tseng, "Efficient construction of robust artificial neural networks for accurate determination of superficial sample optical properties," Biomed. Opt. Express **6**(3), 747–760 (2015).
21. I. Oshina and J. Spigulis J, "Beer-Lambert law for optical tissue diagnostics: current state of the art and the main limitations," J. Biomed. Opt. **26**(10), 100901 (2021).
22. Oregon Medical Laser Center, https://omlc.org/spectra/PhotochemCAD/html/119.html
23. M. Radfar, M. Hashemieh, F. Shirvani, and R. Madani, "Transcutaneous bilirubinometry in preterm and term newborn infants before and during phototherapy," Arch. Iran Med. **19**(5), 323–328 (2016).
24. Z. Kuang, X. Zong, S. Xing, F. Zhao, S. Guo, H. Li, and D. Wei, "Analytical performance validation and clinical application of blood gas analyzer on the detection of neonatal bilirubin," Transl. Pediatr. **10**(12), 3175–3183 (2021).
25. N. Polley, S. Saha, S. Singh, A. Adhikari, S. Das, B. R. Choudhury, and S. K. Pal, "Development and optimization of a noncontact optical device for online monitoring of jaundice in human subjects," J. Biomed. Opt. **20**(6), 067001 (2015).
26. K. L. Newman, K. M. Johnson, P. B. Cornia, P. Wu, K. Itani, and G. N. Ioannou, "Perioperative evaluation and management of patients with cirrhosis: risk assessment, surgical outcomes, and future directions," Clin. Gastroenterol. Hepatol. **18**(11), 2398–2414.e3 (2020).
27. B. M. Fung, M. Perumpail, Y. A. Patel, and J. H. Tabibian, "Telemedicine in hepatology: current applications and future directions," Liver Transpl. **28**(2), 294–303 (2022).

Biomedical Optics EXPRESS

28. P. Alvarez, A. Sianis, J. Brown, A. Ali, and A. Briasoulis, "Chronic disease management in heart failure: focus on telemedicine and remote monitoring," Rev. Cardiovasc. Med. **22**(2), 403–413 (2021).
29. B. L. Cullen, F. Genasi, I. Symington, J. Bagg, M. McCreaddie, A. Taylor, M. Henry, S. J. Hutchinson, and D. J. Goldberg, "Potential for reported needlestick injury prevention among healthcare workers through safety device usage and improvement of guideline adherence: expert panel assessment," J. Hosp. Infect. **63**(4), 445–451 (2006).
30. R. G. Mannino, D. R. Myers, E. A. Tyburski, C. Caruso, J. Boudreaux, T. Leong, G. D. Clifford, and W. A. Lam, "Smartphone app for non-invasive detection of anemia using only patient-sourced photos," Nat. Commun. **9**(1), 4924 (2018).